Editors' Suggestion

Emergence of an optimal temperature in action-potential propagation through myelinated axons

Xinlin Song,[1,2] Hengtong Wang,[3] Yong Chen,[1,2] and Ying-Cheng Lai[4]

[1]*Center of Soft Matter Physics and Its Applications, Beihang University, Beijing 100191, China*

[2]*School of Physics and Nuclear Energy Engineering, Beihang University, Beijing 100191, China*

[3]*School of Physics and Information Technology, Shaanxi Normal University, Xi'an 710119, China*

[4]*School of Electrical, Computer, and Energy Engineering, Arizona State University, Tempe, Arizona 85287, USA*

(Received 16 July 2019; published 30 September 2019)

In biological organisms, an optimal temperature exists at which the system functioning is maximized or is most effective. To obtain a general and quantitative understanding of the emergence of the optimal temperature is a challenging task. We aim to gain insights into this significant problem in biological physics by addressing the problem of propagation of action potential in myelinated axons. In particular, we construct a Hodgkin-Huxley type of cortical, compartmental model to describe the nodes of Ranvier with coupling between a pair of neighboring compartments characterized by internodal conductance and investigate the effect of temperature on the propagation of the action potential. We conduct direct numerical simulations and develop a physical analysis by taking advantage of the spatially continuous approximation. We find that increasing the temperature requires a larger value of the critical internodal conductance for successful propagation. The striking finding is the spontaneous emergence of an optimal temperature in the sense that, for the propagation of a single action potential at a fixed value of the internodal conductance, the minimum average passage time for one node of Ranvier occurs at this temperature value. A remarkable phenomenon is that the value of the optimal temperature is similar to those of living biological systems observed in experiments.

DOI: 10.1103/PhysRevE.100.032416

I. INTRODUCTION

The normal functioning of biological organisms depends critically on the environmental temperature. In biological physics, temperature is thus a fundamental parameter. The existence of a "comfortable" or optimal temperature for any biological system is common knowledge (e.g., the normal human body temperature is about 36 °–37 °C). In spite of experimental evidence and qualitative or heuristic explanations [1–9], at the computational or theoretical level, the emergence of an optimal temperature has not been well understood. Because of the vast complexity of biological systems, to obtain a quantitative understanding is a challenging task. The purpose of this paper is to generate insights into the problem by investigating the concrete problem of action-potential propagation along a myelinated axon. Through constructing and simulating a reasonably detailed compartment model as well as a physical analysis, we find the general existence of an optimal temperature that maximizes the propagation speed.

Myelinated axons play an impotent role in the propagation of action potentials in neural systems [10–13]. Action potentials, often manifested as complex spikes in systems such as the olive fiber and pyramidal cell [14,15], are initiated at the beginning part of the axon and propagate along it. Along the axon, there is a distribution of myelin, by which the action potentials are integrated. The resulting electrical action can modulate the myelin thickness, the length, and the distribution on the axon, leading to white matter and myelinated axon plasticities [16]. An appropriate profile of the myelin distribution along the axon can enhance the synchronous arrival of action potentials [17], and changes in the length and thickness of the myelin sheath can in turn modulate the firing and the conduction velocity of the action potential [18]. Another mechanism to regulate the action potential is through the distribution of ionic channels on the nodes of Ranvier (NoRs) in the axon. Especially, the inactivated Kv1 channels can expand the widths of the action potentials, and de-inactivated Nav channels can enhance the amplitudes of the action potentials to affect the neurotransmitter release in the synaptic gap [19–22]. Myelinated axons are thus an essential component in the integration of the action potentials.

Structurally, a myelinated axon is composed of the NoRs and the myelin sheath, including the paranodal junction, the juxtaparanodes, and the internodal region. Computationally, a myelinated axon can be treated by using a multiple compartment, Hodgkin-Huxley (HH) type of model to describe the membrane potential kinetics of NoRs, which are coupled with internode conductance that decays along the myelin sheath. It was observed from the resonance induced by ion-channel noise that there is an optimal number of ionic channels in the NoRs [23]. In addition, a complicated model was articulated which includes paranodal and myelin attachment compartments to study the myelinated axonal oscillations in developing mammals and the function of internodal sodium channels [24,25]. A remyelinated factor was also proposed to regulate the propagation speed of the action potential in the myelinated axon [26].

The role of temperature in catalytic reactions of biological enzymes and the hydrolysis of ATP was studied quite early [1,2]. In experimental neuroscience, sometimes temperature is more effective at blocking signal conduction in axons than chemical substances. In early experiments, it was observed

that low temperatures could decrease the firing frequency and induce conduction failures in myelinated and unmyelinated axons [27]. Relatively low temperatures are thus useful for improving methods in which high-frequency electrical signals block information propagation along axons to prevent signals with abnormally high electrical level [28]. However, at high temperatures (e.g., fever-like temperatures), the amplitude of the compound action potential in unmyelinated axons in the gray matter decreases, causing a loss of information [29]. It was also demonstrated that, at high temperatures, high-frequency electric signals can block the conduction of action potentials in axons [30]. A model was constructed to explain that the pointwise high-temperature distribution generated by a laser beam can stimulate an axon to produce action potentials [31]. Recently a formula was derived for the conduction velocity of the action potential and its dependence on remyelination [26]. Three models of myelinated axons were articulated to analyze the effect of the myelin sheath [32]. Based on the cable equation theory, the conduction velocity along a myelinated axon was shown to be faster than that along an unmyelinated axon [33]. All these works point at the paramount importance of temperature in the propagation of action potentials along axons, yet the quantitative influence of temperature on spike propagation along myelinated axons has not been well understood.

In this paper, we develop a multicompartment model to study the effect of temperature on spike propagation in myelinated axons. The main result is the following formula for t_p, the time required for a spike to traverse the axon:

$$t_p \simeq \frac{C}{2}\sqrt{\frac{R}{\kappa}}, \tag{1}$$

where C is the membrane capacitance per unit cross-sectional area which has little dependence on temperature, R is the membrane resistance that depends on the ionic channel conductance and the gating probabilities, both being quantities that depend strongly on the temperature, and κ is the internode conductance determined by the geometric and physical properties of the myelinated axon and henceforth is also temperature dependent. We derive Eq. (1) using the approximate theory of spatially continuous cable equation, which indicates that the temperature dependence of the propagation time is determined by a combined effect on the temperature of R and κ. Analysis reveals that the critical internodal intensity for successful propagation increases with the temperature, and the propagation velocity depends on the internodal intensity and thus on the temperature. Both theory and numerics, which agree with each other, give the existence of a critical temperature at which the velocity reaches a maximum. We compare the critical temperature value with those from a number of experiments and find a remarkable consistence. Our results thus establish firmly the existence of an optimal temperature for the concrete problem of signal propagation in myelinated axons with general implications to the temperature constraint in biological functioning and optimization.

II. MODEL

We consider a myelinated axon composed of N coupled HH type of compartments [34]. A schematic illustration of the propagation of the action potential is shown in Fig. 1. The ith node's kinetics can be described by the dynamical evolution of the cortical membrane potentials as

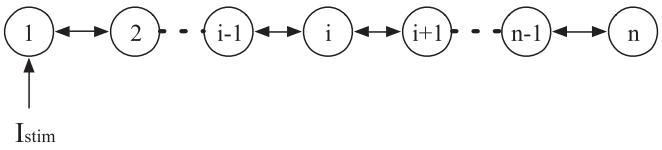

FIG. 1. Schematic diagram of action-potential propagation along a myelinated axon. The NoRs are represented by the numbered circles, the bidirectional arrows denote the myelin sheath, and $I_{\rm stim}$ is the external input.

$$C\frac{dV_i}{dt} = -\bar{g}_{Na}m_i^3h(V_i - V_{Na}) - \bar{g}_K n_i(V_i - V_K) - \bar{g}_L(V_i - V_L) + I_{i,\rm stim} + I_{i,\rm inter}, \tag{2}$$

$$\frac{dm_i}{dt} = \frac{1}{\tau_{m_i}}(-m_i + m_{i,\infty}), \tag{3}$$

$$\frac{dh_i}{dt} = \frac{1}{\tau_{h_i}}(-h_i + h_{i,\infty}), \tag{4}$$

$$\frac{dn_i}{dt} = \frac{1}{\tau_{n_i}}(-n_i + n_{i,\infty}), \tag{5}$$

where V_i is the membrane potential, and m, h, and n are the gating probabilities of different ionic channels. The capacitance is fixed at $C = 0.75\,\mu F/\mathrm{cm}^2$, and the Na^+, K^+, and Cl^- conductances are $\bar{g}_{Na} = 150.0\,\mathrm{mS/cm}^2$, $\bar{g}_K = 40.0\,\mathrm{mS/cm}^2$, and $\bar{g}_L = 0.033\,\mathrm{mS/cm}^2$, respectively. Other parameters are $V_{Na} = 60\,\mathrm{mV}$, $V_K = -90\,\mathrm{mV}$, $V_L = -70\,\mathrm{mV}$, and

$$\tau_{m_i} = \frac{1}{\alpha_{m_i} + \beta_{m_i}}, \quad m_{i,\infty} = \frac{\alpha_{m_i}}{\alpha_{m_i} + \beta_{m_i}}, \tag{6}$$

$$\tau_{h_i} = \frac{1}{\alpha_{h_i} + \beta_{h_i}}, \quad h_{i,\infty} = \frac{1}{1 + e^{(V_i+60)/6.2}}, \tag{7}$$

$$\tau_{n_i} = \frac{1}{\alpha_{n_i} + \beta_{n_i}}, \quad n_{i,\infty} = \frac{\alpha_{n_i}}{\alpha_{n_i} + \beta_{n_i}}, \tag{8}$$

where α_{m_i}, β_{m_i}, α_{h_i}, β_{h_i}, α_{n_i}, and β_{n_i} are defined as

$$\alpha_{m_i} = \phi\frac{0.182(V_i + 30)}{1 - e^{-(V_i+30)/8}}, \quad \beta_{m_i} = -\phi\frac{0.124(V_i + 30)}{1 - e^{(V_i+30)/8}},$$
$$\alpha_{h_i} = \phi\frac{0.028(V_i + 45)}{1 - e^{-(V_i+45)/6}}, \quad \beta_{h_i} = -\phi\frac{0.0091(V_i + 70)}{1 - e^{(V_i+70)/6}},$$
$$\alpha_{n_i} = \phi\frac{0.01(V_i - 30)}{1 - e^{-(V_i-30)/9}}, \quad \beta_{n_i} = -\phi\frac{0.002(V_i - 30)}{1 - e^{(V_i-30)/9}},$$
$$\phi = Q_{10}^{(T-23)/10}. \tag{9}$$

ϕ is an experimentally determined factor characterizing the effect of temperature, and $Q_{10} = 2.3$ is the temperature coefficient. Note that T denotes temperature on the Celsius scale. The internodal current $I_{i,\rm inter}$ is given by

$$I_{i,\rm inter} = \begin{cases} \kappa(V_{i+1} - V_i), & \text{for} \quad i = 0, \\ \kappa(V_{i-1} - V_i), & \text{for} \quad i = N-1, \\ \kappa(V_{i-1} - 2V_i + V_{i+1}), & \text{elsewhere}, \end{cases} \tag{10}$$

where κ is the internodal conductance determined by the geometric and physical characteristics of the myelinated axon,

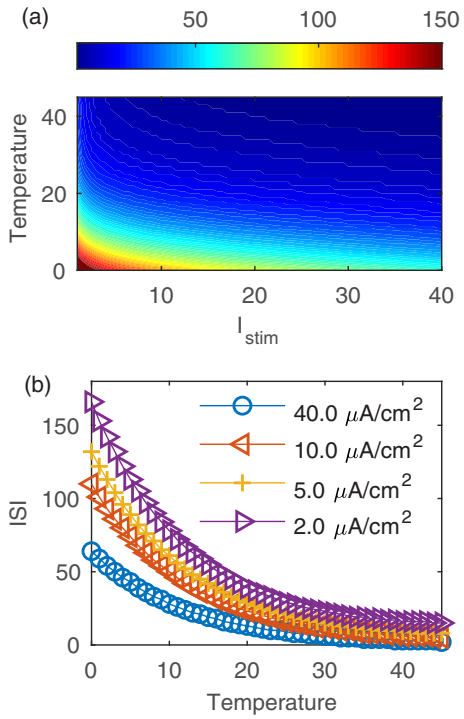

FIG. 2. Interspike intervals (ISIs) of firing patterns of a single neuron. (a) Dependence of ISI on external current $I_{\rm stim}$ in the range from 1 to 40 mA/cm^2. The range of temperature variation is from 0 to 45 °C. (b) Dependence of ISI on temperature for values of $I_{\rm stim}$ = 2.0, 5.0, 10.0, and 40.0 mA/cm^2.

such as the axon diameter, the internodal length, the nodal length, and the cytoplasmic resistivity.

Figure 2 shows the dependence of the interspike interval (ISI) on temperature with increasing external current $I_{\rm stim}$ for a single cortical HH neuron. For any positive value of $I_{\rm stim}$, the cortical HH neuron described by Eq. (2) generates action potentials. Figure 2(a) shows that the ISI decreases with increasing temperature and input DC current. In fact, the neuron is much more sensitive to external currents at low temperatures. Figure 2(b) shows the dependence of ISI on temperature for several different values of $I_{\rm stim}$.

To be concrete, we choose $I_{\rm stim} = 10\,{\rm mA/cm^2}$ to generate spike trains and study their propagation in a myelinated axon. The range of ISI variation is from 100 ms to 10 ms, and the temperature ranges from 0 °C to 45 °C. We use the fourth-order Runge-Kutta algorithm to simulate the HH type of coupled compartment chain model of the axon, with the time step $h = 0.002$. The transient period is approximately 3000 time units, and the initial values are chosen to be $(-59.9, 0.414, 0.095, 0.398)$. In the first 100 time units, the coupling strength κ is 0.0. Then κ is set at the given value. The external current $I_{\rm stim}$ is injected to the first node for 150 time units.

III. RESULTS

A. Propagation of action-potential trains

We consider continuous periodic spike trains induced by a constant direct current, which propagate in the myelinated axon. Figure 3 shows the propagation of action-potential trains for different values of the internodal conductance κ at temperatures $T = 15\,^\circ$C and 23 °C. The spike trains are triggered at the first NoR, but the firing frequencies at low temperatures (upper panels) are larger than those at high temperatures (bottom panels). This is consistent with the firing behaviors of a single NoR (Fig. 2). For weak coupling conductance [Figs. 3(a), 3(e), and 3(f)], no action potential can reach the last 50th NoR. With increasing values of κ, the action-potential trains pass through the axon partially [Figs. 3(b) and 3(c) and 3(g)] or completely [Figs. 3(d) and 3(h)].

The behaviors of propagation of spikes as illustrated in Fig. 3 indicate that there are two critical values of temperature-dependent internodal conductance, corresponding to transmission κ_{c1} and complete transmission κ_{c2}, where κ_{c1} means that spike propagation occurs [Figs. 3(b) and 3(g)], while κ_{c2} signifies that the spikes can propagate through the myelinated axon [Figs. 3(d) and 3(h)]. Figure 4(a) shows the ratio between the spike counts at the terminal NoR and the first NoR for different values of the temperature T and internodal conductance κ. Note that the white region denotes the case where there is no firing at the end NoR or that the propagation is totally blocked. Both critical values of κ increase with the temperature. For example, as shown in Fig. 4(b), we have $\kappa_{c1} = 0.0562, 0.1343, 0.3212$, and $\kappa_{c2} = 0.1923, 0.3051, 0.5944$ for $T = 20\,^\circ$C, 30 °C, and 40 °C, respectively. If the internodal conductance value κ is smaller than κ_{c1} [the white area in Fig. 4(a)], no action potential is triggered at the terminal NoR. For $\kappa_{c1} < \kappa < \kappa_{c2}$ [the narrow area between the white and red areas in Fig. 4(a)], the spike sequence appears at the final NoR, but some spikes are still missing. For $\kappa > \kappa_{c2}$ [the red area in Fig. 4(a)], the fraction of the spikes that pass the axon increases to one, indicating that all spikes generated at the initial NoR transit successfully the 50-node-long myelinated axon.

Similarly, two critical temperature values arise for a given value of the internodal conductance: T_{c1} for the emergence of transmission and T_{c2} for complete transmission. For $\kappa \lesssim 0.109$, only incomplete transmission has occurred (T_{c1} only), as shown in Fig. 4(a). The κ-dependent critical temperatures for $\kappa = 0.2024, 0.3934$, and 0.5944 are shown in Fig. 4(c). An increase in the temperature drives the spike passing fraction from one in the middle region to zero [from the red complete propagation region to the totally blocked white region in Fig. 4(a)]. This behavior of propagation is qualitatively consistent with the phenomenon of nerve heat block.

B. Propagation of an action potential

Figures 3(b) and 3(d) and 3(g) and 3(h) demonstrate that the propagation times of the action potentials are different, indicating differences in the propagation velocity along the myelinated axon. To study the issue of propagation time (or velocity), we consider a single action potential propagating in the axon containing 50 NoRs. Under a 5 ms-duration $I_{\rm stim} = 10\,{\rm mA/cm^2}$ input pulse, the first node generates one action potential at $t = 150$, which will propagate along the axon.

Figure 5 illustrates the propagation of one action potential at temperatures $T = 15\,^\circ$C and 23°C for different values of

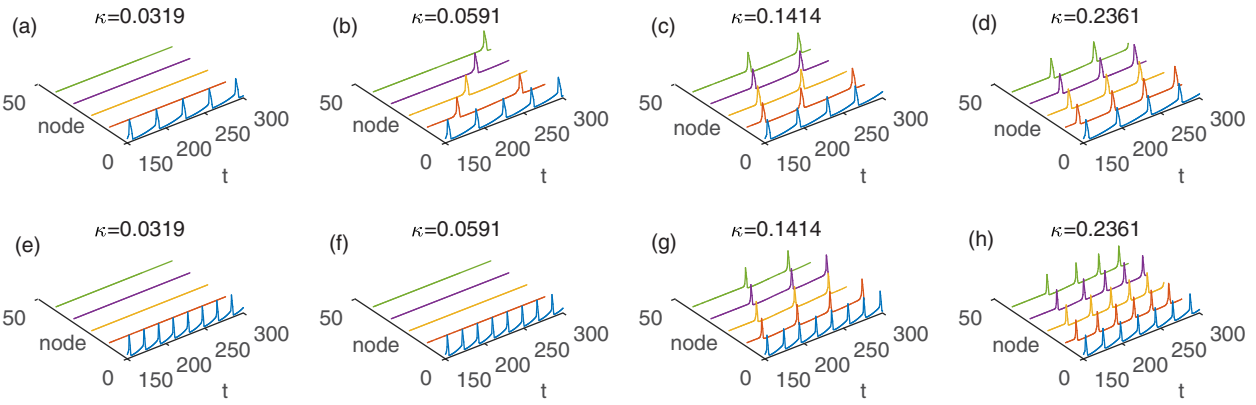

FIG. 3. Propagation of a train of action potentials. The axon contains $N = 50$ NoRs with $I_{\text{stim}} = 10\,\text{mA/cm}^2$. Shown are the results for different values of temperature: (a–d) $T = 15\,^\circ\text{C}$ and (e–h) $T = 23\,^\circ\text{C}$.

the internodal conductances κ. While the action potentials can successfully propagate through the entire axon for $\kappa > \kappa_{c1}$, the arrival times at the end of the axon are different and depend on both the temperature and the conductance values, as shown in Figs. 5(b) and 5(d), 5(c) and 5(g), and 5(d) and 5(h).

Using the same protocol as that for the propagation of a single spike in a myelinated axon, we carry out extensive simulations to reveal the dependencies of the velocity on temperature T and internodal conductance κ, as shown in Fig. 6(a), where the white regions correspond to those in which the spike fails to propagate the axon. The results indicate that, at higher temperatures, larger values of κ are required for successful spike transmission through the myelinated axon. In Fig. 6(a) the color bar denotes the average passage time t_p through one NoR, and the contour plots indicate that the value of t_p decreases (or the propagation velocity increases) as the value of κ is increased for any given temperature T. The remarkable phenomenon is that, for a fixed value of κ, t_p does not depend on the temperature monotonously. In particular, as T is increased from zero, the value of t_p decreases, reaches a minimum, and then increases, signifying the existence of an optimal temperature value at which the propagation speed is maximized. At the optimal temperature, there is rapid propagation of the action potential through the myelinated axon.

Our use of the HH type of equation to model the NoR and the fact that the myelin sheath can be quantitatively described by the internodal conductance κ (cf. Fig. 1) justify a continuous approximation for the spatially discrete ODE model. The details are given in the Appendix. Analyzing the spatially continuous model, we arrive at the main quantitative result Eq. (1). The results of this theoretical formula are displayed in Fig. 6(b), where the average passage time of a spike is plotted as a function of T and κ. Comparing with the directly simulated results in Fig. 6(a), we obtain a reasonable agreement.

Figure 7 shows the minimal average passage times of a spike through one NoR and the corresponding optimal temperature value as a function of the internodal conductance κ. Both the simulation results and the theoretical prediction of Eq. (1) indicate that the minimal propagation time decreases and the corresponding optimal temperature increases monotonically

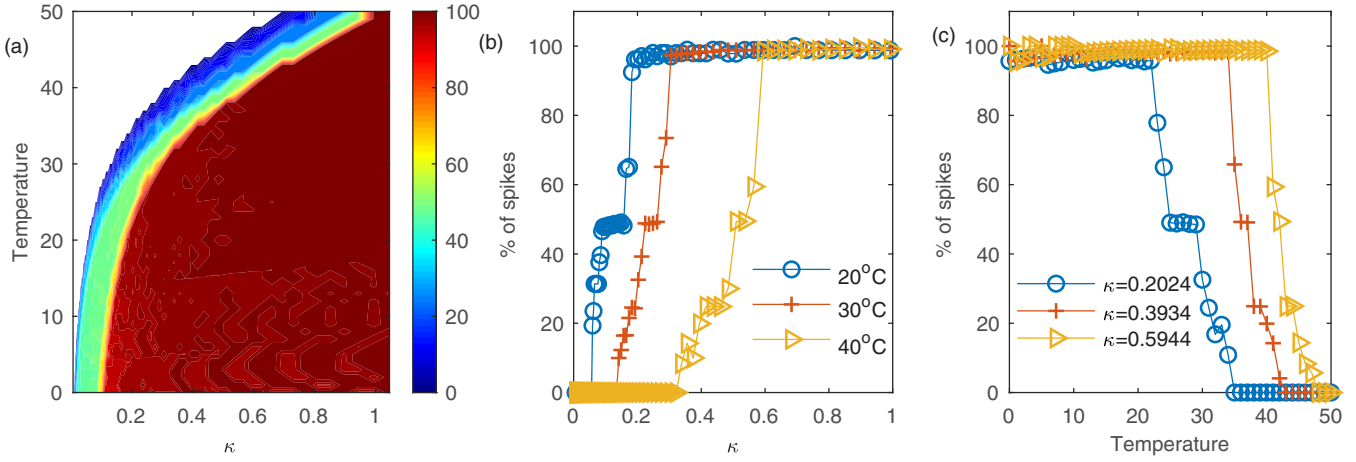

FIG. 4. Fraction of spikes successfully propagating along the entire axon. (a) Color-coded fraction in the parameter plane of temperature T and internodal conductance κ, (b) the fraction versus κ for three temperature values, and (c) the fraction versus T for three values of κ. The input is $I_{\text{stim}} = 10\,\text{mA/cm}^2$, and the number of NoRs is $N = 50$.

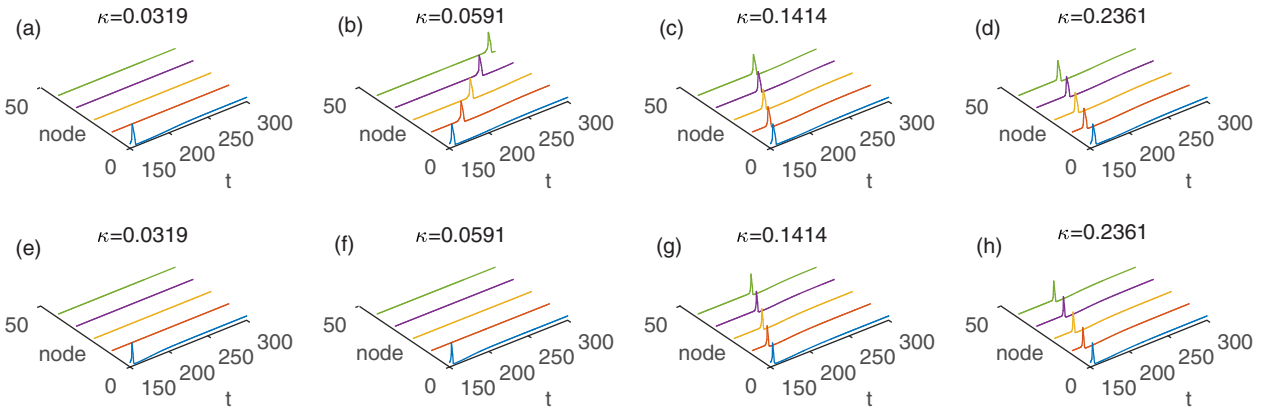

FIG. 5. Propagation of a single action potential. The axon contains $N = 50$ NoRs. The temperature values are (a–d) $T = 15\,^{\circ}\mathrm{C}$ and (e–h) $23\,^{\circ}\mathrm{C}$. With the input pulse $I_{\mathrm{stim}} = 10\,\mathrm{mA/cm^2}$, 5 ms is required to generate only one action potential at the first NoR.

with κ. The predictions of Eq. (1) are qualitatively consistent with the simulation result. Table I lists some relevant experimental data of spike propagation along the axon. By calculating the value of the internodal conductance κ, we can get the optimal temperature value for minimal propagation time through direct simulations and Eq. (1). Strikingly, the temperature values are quire similar to those from experiments, as indicated in Table I and the black stars in Fig. 7.

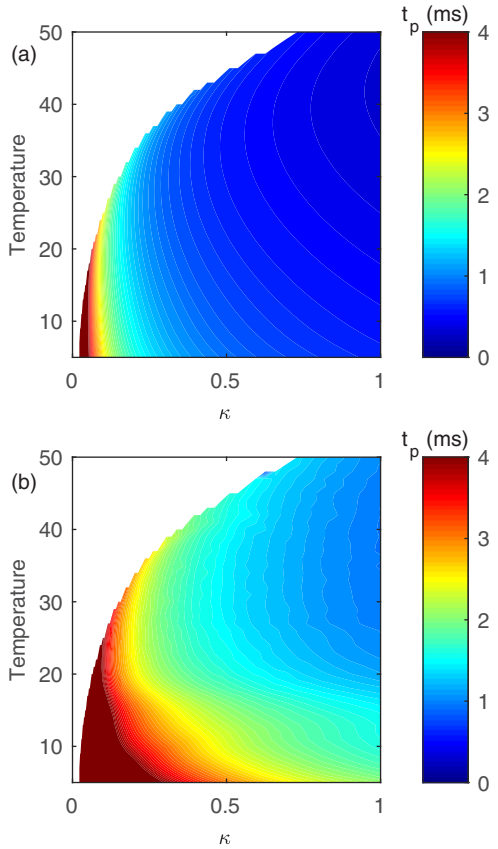

FIG. 6. Average passage time through one NoR associated with single-spike propagation. The axon has 50 nodes. The results are based on (a) simulations with Eqs. (2)–(10) and (b) an approximate theory of the continuous cable equation [Eq. (1)]. The unit of the average passage time is indicated on the top of the color bar in each panel.

IV. DISCUSSION

In this work, motivated by the lack of a general understanding of the existence of an optimal temperature of functioning for a large variety of biological systems, we study the effect of temperature on the propagation of action potential along a myelinated axon. Our simulation results and a physical analysis suggest that inappropriate values of temperature can block spike propagation and an optimal temperature does exist to maximize the propagation velocity.

For spike trains, a previous work [23] showed that the fraction between the number of action potentials at the end NoR and that of the input exhibits distinct patterns as the value of the internodal conductance κ is increased. We have observed that the critical value of κ for propagation increases

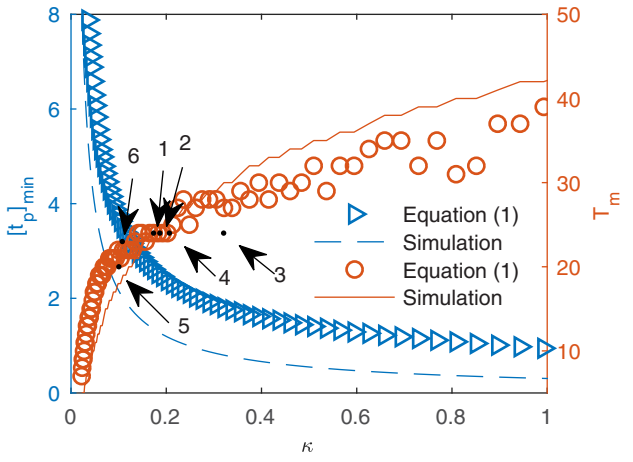

FIG. 7. Dependence of optimal temperature on internodal conductance. Shown are the minimal average time of a single action potential propagating through one NoR and the corresponding temperature T_m as a function of the internodal conductance κ. The blue dashed and red solid curves are the simulation results. The blue triangles and red circles are the prediction from Eq. (1). The black solid circles represent the data in Table I.

TABLE I. Relevant experimental results of spike propagation in a myelinated axon

Label		d (μm)	R_c (Ωcm)	l (μm)	μ (μm)	Temperature (°C)			$\kappa = \frac{d}{4R_c l\mu}$
						Experiment	Simulation	Eq. (1)	
1	Rat optic nerve [18]	0.73	70	139.26	1.08	24[a]	23.3	24	0.1733
2	Rat cortex [18]	0.64	70	81.7	1.5	24[a]	24.1	25.3	0.1865
3	Rat GBC lateral [19]	1.68	70	187.2	1.0	24	29.3	28.6	0.3205
4	Frog [35]	20	110	2200	1.0	24[a]	25.1	25.9	0.2066
5	Rat model [36]	10	166	1000	1.5	20	17.8	21.1	0.1004
6	*Xenopus laevis* model [37]	0.7D[b]	65	100D[b]	2.5	23	18.5	21.5	0.1077

[a]Room temperature.
[b]D is the diameter of the axon.

with the temperature. There were also previous results that the speed of spike propagation increases monotonically with the environmental temperature [27,37,38]. However, the temperature ranges in these studies were narrow. Distinct from the previous studies, we have found that the average passage time through one NoR decreases and then increases with increasing temperature (Fig. 6), stipulating the existence of an optimal temperature warranting the fastest possible spike propagation under the circumstances (Fig. 7). A remarkable observation is that the optimal temperature values are similar to those in a number of experiments (Table I).

We have employed a Hodgkin-Huxley type of cortical model to describe the kinetics of the NoR in the myelinated axon, which is justified by previous biological experiments [34]. Utilizing a continuous spatial description of the cable equation to approximate the spatially discrete compartment model used in the simulations, we obtain that the average passage time is determined mainly by the membrane resistance R for a fixed value of the internodal conductance κ [Eq. (1)]. In general, R depends on the state of the ionic channels, which is greatly influenced by the temperature. A higher temperature is beneficial to ionic movements but, at the same time, leads to greater thermal fluctuations in the structure of the channels. The emergence of an optimal temperature is the result of these two competing factors, at which the propagation is the fastest. It is quite striking that the optimal temperature values are similar to the living temperatures of the species resulting from evolution and adaptation. We note that, in a recent paper [39], it was demonstrated through a combined analysis of cross-covariance, information entropy, and mutual information of spike trains that, to maintain the normal body temperature in the optimal range $36^\circ - 38\,^\circ$C is essential for reliable and effective information processing in rodent cortical neurons, which corroborates our result. Our finding has implications for the consequences of global warming that may force biological organisms to operate at extreme temperatures [40].

ACKNOWLEDGMENTS

This work was supported by the National Natural Science Foundation of China under Grants No. 11675008, No. 21434001, and No. 11447027. H.T.W. acknowledges additional supports from the Fundamental Research Funds for the Central Universities under Grant No. GK201503025 and the Natural Science Basic Research Plan in Shaanxi Province of China under Grant No. 2016JQ1037. Y.C.L. is supported by the Office of Naval Research through Grant No. N00014-16-1-2828.

APPENDIX: PROPAGATION OF AN ACTION POTENTIAL IN THE MYELINATED AXON

When an action potential propagates in a myelinated axon as schematically demonstrated in Fig. 1, the current between the $(n-1)$th node and the neighboring nth node is given by

$$i_n = -\frac{\pi d^2}{4R_c}\frac{\partial V}{\partial x} = \frac{\pi d^2}{4R_c l}(V_{n-1} - V_n), \tag{A1}$$

where l is the internodal length, d is the axon diameter, μ is the node length, and R_c is the cytoplasmic resistivity of the axon. Using the definition of the HH-type NoR (2), we obtain, for the nth node,

$$\mu\pi d\left(C\frac{\partial V_n}{\partial t} + I_{\text{ion}}\right) = i_n - i_{n+1} = \frac{\pi d^2}{4R_c l}(V_{n+1} - 2V_n + V_{n-1}),$$

$$C\frac{\partial V_n}{\partial t} + I_{\text{ion}} = \kappa(V_{n+1} - 2V_n + V_{n-1}), \tag{A2}$$

where the internodal conductance is $\kappa = d/(4R_c l\mu)$ and the electric current in the membrane ionic channels is I_{ion}. We approximate this equation by

$$C\frac{\partial V(\mathrm{x},t)}{\partial t} + I_{\text{ion}} = \kappa[V(x+\Delta x,t) - 2V(x,t) + V(x-\Delta x,t)], \tag{A3}$$

where Δx is the distance between two neighboring NoRs. In the spatially continuous form, this equation becomes

$$C\frac{\partial V(x,t)}{\partial t} + I_{\text{ion}} = \kappa\left(\left.\frac{\partial V}{\partial x}\right|_{x,t} - \left.\frac{\partial V}{\partial x}\right|_{x-\Delta x,t}\right)\Delta x,$$

$$C\frac{\partial V}{\partial t} + I_{\text{ion}} = \kappa\left(\frac{\partial^2 V}{\partial x^2}\right)\Delta x^2. \tag{A4}$$

By defining the membrane resistivity in the NoR: $R = V/I_{\text{ion}} = V/(I_{Na} + I_K + I_{Cl})$, we rewrite this equation as

$$CR\frac{\partial V}{\partial t} + V = \kappa R\Delta x^2\frac{\partial^2 V}{\partial x^2}$$

or

$$\tau\frac{\partial V}{\partial t} + V = \lambda^2\frac{\partial^2 V}{\partial x^2}, \tag{A5}$$

where $\tau = CR$ and $\lambda = \sqrt{\kappa R}\Delta x$.

With the input current on the left starting point given by $I_{\rm stim}(x,t) = I_0\delta(x)\delta(t)$, we have that the membrane potential of the NoR is given by

$$\tau\frac{\partial V}{\partial t} + V - \lambda^2\frac{\partial^2 V}{\partial x^2} = RI_0\delta(x)\delta(t). \tag{A6}$$

Taking the Fourier transformation

$$\widehat{V}(k,t) = \int_{-\infty}^{\infty} e^{-ikx}V(x,t)\,dx,$$

$$\widehat{I}(k,t) = \int_{-\infty}^{\infty} e^{-ikx}I_{\rm stim}(x,t)\,dx,$$

we obtain Eq. (A6) in the Fourier space as

$$\tau\frac{d\widehat{V}}{dt} + (1+\lambda^2k^2)\widehat{V} - R\widehat{I} = 0, \tag{A7}$$

with its solution given by

$$\widehat{V}(k,t) = \widehat{V}_0(k)e^{-\frac{1}{\tau}(1+\lambda^2k^2)t} + \frac{R}{\tau} \times \int_0^t e^{-\frac{1}{\tau}(1+\lambda^2k^2)(t-s)}\widehat{I}_{\rm stim}(k,s)\,ds, \tag{A8}$$

where $\widehat{V}_0(k)$ denotes the Fourier form of the initial state. Taking the inverse Fourier transformation, we obtain

$$V(x,t) = \frac{RI_0}{\tau\lambda\sqrt{4\pi t/\tau}}\exp\left(-\frac{\tau x^2}{4\lambda^2 t} - \frac{t}{\tau}\right). \tag{A9}$$

The local extreme is the peak position in an action potential. Taking the time derivative of Eq. (A9), we get

$$\frac{dV(x,t)}{dt} = \frac{I_0R}{8\sqrt{\pi}\lambda^3\tau^{3/2}}\frac{-2\lambda^2t(2t+\tau)+\tau^2x^2}{t^{3/2}} \times \exp\left(-\frac{\tau x^2}{4\lambda^2 t} - \frac{t}{\tau}\right). \tag{A10}$$

Setting $dV(x,t)/dt = 0$, we obtain the time t_m that $V(x,t)$ reaches the maximum at position x as

$$t_m = \frac{\tau}{4}\left[\sqrt{1+4(x/\lambda)^2} - 1\right]. \tag{A11}$$

Inserting $x = N\Delta x$, $\tau = CR$, and $\lambda = \sqrt{\kappa R}\Delta x$ into this expression, we obtain the arrival time of the spike at the Nth node:

$$t_m = \frac{\tau}{4}\left[\sqrt{1+4\left(\frac{N\Delta x}{\lambda}\right)^2} - 1\right] = \frac{CR}{4}\left(\sqrt{1+\frac{4N^2}{\kappa R}} - 1\right). \tag{A12}$$

Consequently, the average passage time of a spike through one node t_p is given by

$$t_p = \frac{t_m}{N} = \frac{CR}{4N}\left(\sqrt{1+\frac{4N^2}{\kappa R}} - 1\right) \simeq \frac{C}{2}\sqrt{\frac{R}{\kappa}}. \tag{A13}$$

[1] J. K. Raison, The influence of temperature-induced phase changes on the kinetics of respiratory and other membrane-associated enzyme systems, J. Bioenerg. **4**, 285 (1973).

[2] G. N. Somero, Temperature adaptation of enzymes: Biological optimization through structure-function compromises, Ann. Rev. Ecol. Syst. **9**, 1 (1978).

[3] R. J. Rowbury, Temperature effects on biological systems: Introduction, Sci. Prog. **86**, 1 (2003).

[4] M. E. Peterson, R. M. Daniel, M. J. Danson, and R. Eisenthal, The dependence of enzyme activity on temperature: Determination and validation of parameters, Biochem. J. **402 (Pt. 2)**, 331 (2007).

[5] A. I. Dell, S. Pawar, and V. M. Savage, Systematic variation in the temperature dependence of physiological and ecological traits, Proc. Natl. Acad. Sci. U. S. A. **108**, 10591 (2011).

[6] L. A. Schipper, J. K. Hobbs, S. Rutledge, and V. L. Arcus, Thermodynamic theory explains the temperature optima of soil microbial processes and high Q_{10} values at low temperatures, Global Change Biol. **20**, 3578 (2014).

[7] P. M. Schulte, The effects of temperature on aerobic metabolism: Towards a mechanistic understanding of the responses of ectotherms to a changing environment, J. Exp. Biol. **218**, 1856 (2015).

[8] M. L. Begasse, M. Leaver, F. Vazquez, S. W. Grill, and A. A. Hyman, Temperature dependence of cell division timing accounts for a shift in the thermal limits of C. elegans and C. briggsae, Cell Rep. **10**, 647 (2015).

[9] V. L. Arcus, E. J. Prentice, J. K. Hobbs, A. J. Mulholland, M. W. V. der Kamp, C. R. Pudney, E. J. Parker, and L. A. Schipper, On the temperature dependence of enzyme-catalyzed rates, Biochemistry **55**, 1681 (2016).

[10] D. Debanne, Information processing in the axon, Nat. Rev. Neurosci. **5**, 304 (2004).

[11] G. A. Mihailoff and D. E. Haines, The cell biology of neurons and glia, in *Fundamental Neuroscience for Basic and Clinical Applications*, 5th ed., edited by D. E. Haines and G. A. Mihailoff (Elsevier, Philadelphia, PA, 2018), Chap. 2, pp. 15–33.e1.

[12] M. H. Kole and G. J. Stuart, Signal processing in the axon initial segment, Neuron **73**, 235 (2012).

[13] M. H. P. Kole, S. U. Ilschner, B. M. Kampa, S. R. Williams, P. C. Ruben, and G. J. Stuart, Action potential generation requires a high sodium channel density in the axon initial segment, Nat. Neurosci. **11**, 178 (2008).

[14] A. Mathy, S. S. Ho, J. T. Davie, I. C. Duguid, B. A. Clark, and M. Häusser, Encoding of oscillations by axonal bursts in inferior olive neurons, Neuron **62**, 388 (2009).

[15] M. H. Kole, First node of Ranvier facilitates high-frequency burst encoding, Neuron **71**, 671 (2011).

[16] C. Sampaio-Baptista and H. Johansen-Berg, White matter plasticity in the adult brain, Neuron **96**, 1239 (2017).

[17] M. Baraban, S. Mensch, and D. A. Lyons, Adaptive myelination from fish to man, Brain Res. **1641**, 149 (2016).

[18] I. L. Arancibia-Cárcamo, M. C. Ford, L. Cossell, K. Ishida, K. Tohyama, and D. Attwell, Node of Ranvier length as a potential regulator of myelinated axon conduction speed, eLife **6**, e23329 (2017).

[19] M. C. Ford, O. Alexandrova, L. Cossell, A. Stange-Marten, J. Sinclair, C. Kopp-Scheinpflug, M. Pecka, D. Attwell, and

B. Grothe, Tuning of Ranvier node and internode properties in myelinated axons to adjust action potential timing, Nat. Commun. **6**, 8073 (2015).

[20] S. Rama, M. Zbili, and D. Debanne, Signal propagation along the axon, Curr. Opin. Neurobiol. **51**, 37 (2018).

[21] S. Rama, M. Zbili, A. Bialowas, L. Fronzaroli-Molinieres, N. Ankri, E. Carlier, V. Marra, and D. Debanne, Presynaptic hyperpolarization induces a fast analogue modulation of spike-evoked transmission mediated by axonal sodium channels, Nat. Commun. **6**, 10163 (2015).

[22] A. Bialowas, S. Rama, M. Zbili, V. Marra, L. Fronzaroli-Molinieres, N. Ankri, E. Carlier, and D. Debanne, Analog modulation of spike-evoked transmission in CA3 circuits is determined by axonal kv1.1 channels in a time-dependent manner, Eur. J. Neurosci. **41**, 293 (2014).

[23] A. Ochab-Marcinek, G. Schmid, I. Goychuk, and P. Hänggi, Noise-assisted spike propagation in myelinated neurons, Phys. Rev. E **79**, 011904 (2009).

[24] S. Zeng and P. Jung, Axonal oscillations in developing mammalian nerve axons, Phys. Rev. E **71**, 011910 (2005).

[25] S. Zeng and P. Jung, Simulation analysis of intermodal sodium channel function, Phys. Rev. E **78**, 061916 (2008).

[26] A. Scurfield and D. C. Latimer, A computational study of the impact of inhomogeneous internodal lengths on conduction velocity in myelinated neurons, PLoS ONE **13**, e0191106 (2018).

[27] D. N. Franz and A. Iggo, Conduction failure in myelinated and non-myelinated axons at low temperatures, J. Physiol. **199**, 319 (1968).

[28] D. M. Ackermann, E. L. Foldes, N. Bhadra, and K. L. Kilgore, Nerve conduction block using combined thermoelectric cooling and high frequency electrical stimulation, J. Neurosci. Meth. **193**, 72 (2010).

[29] D. Pekala, H. Szkudlarek, and M. Raastad, Typical gray matter axons in mammalian brain fail to conduct action potentials faithfully at fever-like temperatures, Physiol. Rep. **4**, e12981 (2016).

[30] C. Tai, J. Wang, J. R. Roppolo, and W. C. de Groat, Relationship between temperature and stimulation frequency in conduction block of amphibian myelinated axon, J. Comp. Neurosci. **26**, 331 (2008).

[31] S. Fribance, J. Wang, J. R. Roppolo, W. C. de Groat, and C. Tai, Axonal model for temperature stimulation, J. Comp. Neurosci. **41**, 185 (2016).

[32] A. G. Richardson, C. C. McIntyre, and W. M. Grill, Modelling the effects of electric fields on nerve fibres: Influence of the myelin sheath, Med. Biol. Eng. Comp. **38**, 438 (2000).

[33] G. B. Ermentrout and D. H. Terman, *Mathematical Foundations of Neuroscience* (Springer, New York, 2010).

[34] Y. Yu, Y. Shu, and D. A. McCormick, Cortical action potential backpropagation explains spike threshold variability and rapid-onset kinetics, J. Neurosci. **28**, 7260 (2008).

[35] P. Shrager, Ionic channels and signal conduction in single remyelinating frog nerve fibres, J. Physiol. **404**, 695 (1988).

[36] A. Blight, Computer simulation of action potentials and afterpotentials in mammalian myelinated axons: The case for a lower resistance myelin sheath, Neuroscience **15**, 13 (1985).

[37] Z. Mou, I. F. Triantis, V. M. Woods, C. Toumazou, and K. Nikolic, A simulation study of the combined thermoelectric extracellular stimulation of the sciatic nerve of the *Xenopus laevis*: The localized transient heat block, IEEE Trans. Biomed. Eng. **59**, 1758 (2012).

[38] N. A. Hutchinson, Z. J. Koles, and R. S. Smith, Conduction velocity in myelinated nerve fibres of Xenopus laevis, J. Physiol. **208**, 279 (1970).

[39] X. Fu and Y. G. Yu, Reliable and efficient processing of sensory information at body temperature by rodent cortical neurons, Nonlinear Dyn. 1 (2019), doi: 10.1007/s11071-019-05184-2.

[40] L. B. Buckley and R. B. Huey, How extreme temperatures impact organisms and the evolution of their thermal tolerance, Integr. Comp. Biol. **56**, 98 (2016).